Imaging Biomolecule Arrays by Atomic Force Microscopy

Laura T. Mazzola and Stephen P. A. Fodor
Affymetrix, Santa Clara, California 95051 USA

ABSTRACT We describe here a method for constructing ordered molecular arrays and for detecting binding of biomolecules to these arrays using atomic force microscopy (AFM). These arrays simplify the discrimination of surface-bound biomolecules through the spatial control of ligand presentation. First, photolithography is used to spatially direct the synthesis of a matrix of biological ligands. A high-affinity binding partner is then applied to the matrix, which binds at locations defined by the ligand array. AFM is then used to detect the presence and organization of the high-affinity binding partner. Streptavidin-biotin arrays of 100 × 100 μm and 8 × 8 μm elements were fabricated by this method. Contact and noncontact AFM images reveal a dense lawn of streptavidin specific to the regions of biotin derivatization. These protein regions are characterized by a height profile of ~40 Å over the base substrate with a 350-nm edge corresponding to the diffraction zone of the photolithography. High resolution scans reveal a granular topography dominated by 300 Å diameter features. The ligand-bound protein can then be etched from the substrate using the AFM tip, leaving an 8 Å shelf that probably corresponds to the underlying biotin layer.

INTRODUCTION

Detection and characterization of molecular recognition is central to the understanding of many biochemical processes. Conventional detection techniques (e.g., fluorescence tagging and radiolabeling) require chemical modification of one of the partners of the complex. These modifications can subtly alter molecular interactions by changing the chemical nature of the receptor/ligand interaction. Moreover, these methods do not detect single molecular events; instead they sample a broad distribution of molecular interactions with a range of binding parameters.

Atomic force microscopy (AFM) provides a means of sampling molecular interactions. By directly mapping the molecular topography, this technique probes structure and organization without the need for chemical modification (Binnig et al., 1986; Hansma et al., 1988). Until recently, AFM has not been a practical tool for imaging biological samples without significant disruption of the biological structure. This problem has been overcome by techniques that reduce the tip force applied to the sample. High resolution images of biological structures can now be obtained by scanning in solution (Drake et al., 1989; Weisenhorn et al., 1989) and through "noncontact" AFM techniques (Martin et al., 1987; Wiegräbe et al., 1991; Hartmann, 1992). The latter approach exerts orders of magnitude less force on the sample than contact AFM. In addition, advances in tip fabrication have resulted in a more refined tip profile, which enhances the spatial resolution of large structures (Zenhausern et al., 1993). With these developments, AFM has emerged as an instrument to investigate biological systems at the molecular level.

Received for publication 20 October 1994 and in final form 21 February 1995.

Address reprint requests to Laura Mazzola, Affymetrix, 3380 Central Expwy., Santa Clara, CA 95051. Tel.: 408–522–6020; Fax: 408–481–0422; E-mail: lmazzo@affymetrix.com.

0006-3495/95/05/1653/08 $2.00

The challenges associated with detection of biomolecules by AFM can be catagorized as follows (Blackford et al., 1991; Radmacher et al., 1992; Keller and Bustamante, 1993). The molecules must be anchored to a relatively flat surface and should remain firmly bound during scanning. To minimize scan artifacts, the underlying substrate should be rigid with respect to the scanning tip. To clearly identify the molecular species, one would like to control the density, orientation, and spatial distribution of the molecules of interest. Various techniques have been used to immobilize biological samples to a solid support (usually cleaved mica), e.g., protein adsorption from solution (Lin et al., 1990), protein fusion with lipids to form planar membranes (Weisenhorn et al., 1990), DNA linked to gold particles (Shaiu et al., 1993), protein incorporation of a metal-chelating peptide (Ill et al., 1993), and random crosslinking of samples to photoactivated glass (Karrasch et al., 1993). Although these methods have been listed by increasing control of stability and orientation, none offer substantial control of the aforementioned parameters.

We have prepared a more ideal substrate for immobilization and detection of surface-bound biomolecules using techniques that allow light-directed, site-specific synthesis or attachment of biological ligands to a two-dimensional support (Fodor et al., 1991, Pease et al., 1994). By this method, the covalently attached ligand determines the location and orientation of its high affinity binding partner. We present here the techniques for fabrication of spatially-defined biotin arrays and detection of streptavidin binding using AFM.

MATERIALS AND METHODS

Preparation of biomolecule arrays

The molecular arrays were prepared in three steps, illumination of a photoprotected substrate to activate an array of sites, coupling of biotin to the activated array, and incubation with streptavidin. This process is illustrated in Fig. 1, where a checkerboard-patterned lithographic mask was used to activate the surface. This pattern simplifies the discrimination of surface-bound biomolecules from the background substrate by including a negative control for protein binding within the AFM scan.

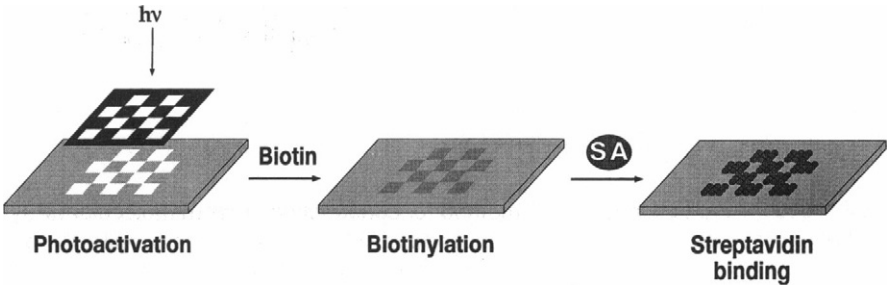

FIGURE 1 Protein arrays were prepared in a three-step process: selective photoactivation of the substrate, biotinylation of the activated array, and incubation of streptavidin with the biotin array. To ensure unambiguous identification of the protein species, a checkerboard illumination pattern was used to activate the substrate. This pattern provides a positive and negative control for protein binding within an AFM scan.

The photoprotected substrates were prepared by cleaning 1.5 mm thick, 3 × 3 inch glass in concentrated NaOH, followed by exhaustive rinsing in water. The surface was then derivatized for 2 h with a solution of 10% (v/v) bis(2-hydroxyethyl)aminopropyltriethoxysilane (Petrarch Chemicals, Bristol, PA) in 95% ethanol, rinsed with ethanol and ether, and dried in vacuo at 40°C. Using standard oligonucleotide synthesis protocols (Atkinson and Smith, 1984), the silanized surface was then reacted with a 50–100 nM solution of 1-*O'*-(α-methyl-6-nitropiperonyloxycarbonyl)-hexaethylene glycol-17-*O*-(*N*,*N*-diisopropylamino)-cyanoethylphosphoramidite (MeNPOC-PEG-CEP):

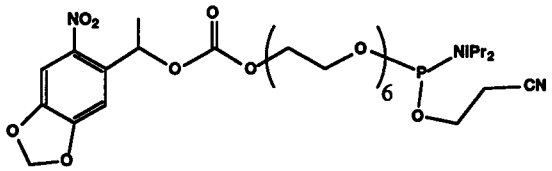

(1)

The MeNPOC protecting group is stable in a variety of solvents, but can be removed by irradiation with 365 nm light. The MeNPOC-PEG linker (PEG: 719 mol wt, United Chemical Technologies, Bristol, PA) was synthesized using a modification of the process described in Pease et al., 1994 (G. McGall and A. D. Barone, in preparation).

The photoprotected substrate was then placed over an index-matched UV-absorbing filter, then covered by the checkerboard-patterned lithographic mask (Photosciences, Torrence, CA). The lithographic masks consists of chrome-on-glass checkerboard patterns with elements ranging in size from 100 × 100 μm to 2 × 2 μm. Substrates were illuminated through the mask for 20 s with 10 mW/cm^2 of the 365-nm output of a Mercury-Xenon arc lamp (Optical Associates, Inc., Milpitas, CA). Under these conditions, a 20-s photolysis deprotects approximately half of the sites within the exposed areas ($t_{1/2} \sim 20$ s), producing free hydroxyl groups of ~100 Å average spacing (~10^4 sites/μm^2). (The density of sites on the substrate has been calculated from experiments using quantitative fluorescence, radiolabeling, and colorimetry techniques, including current studies using photocleavable fluorescent tags (G. McGall and A. D. Barone, in preparation). These techniques derive an intermolecular distance of 20–100 Å. The typical value for site spacing is 50 Å.)

Using the synthesis protocol mentioned above, biotin phosphoramidite (Pharmacia, Alameda, CA) was coupled to the photodeprotected regions of the substrate. After phosphite oxidation, the substrate was deprotected in 5% TCA/DCM to remove the *O*-monomethoxytrityl protecting group. A final full-surface photolysis (220 s) was performed to remove all remaining protecting groups. Finally, the biotin arrays were rinsed with acetonitrile and dried with filtered nitrogen. These ligand substrates were stable for at least several weeks when stored in a dark desiccator.

The biotin arrays were incubated with a 100 μg/ml solution of fluorescein-streptavidin (FITC-SA; Molecular Probes, Eugene, OR) in phosphate-buffered saline (PBS, pH 7.4) with 0.05% Tween for 2 h at room temperature, then agitated for 2 h in PBS/Tween to remove nonspecifically bound protein. Binding assays indicate that these conditions saturate the available binding sites (data not shown). The protein arrays were rinsed with deionized water and dried with filtered nitrogen before imaging. To confirm the presence of surface-bound protein, the arrays were examined with a confocal scanning microscope (Zeiss Axioskop 20, Oberkochen, Germany), using 488 nm excitation light from an argon ion laser to excite the protein-bound fluorescein.

AFM imaging

Atomic force images were obtained with an AutoProbe CP (Park Scientific Instruments, Sunnyvale, CA) equipped with a 100 μm scanning stage and contact/noncontact scanning capability. The protein arrays were scanned at ambient temperature and humidity. Images were acquired at 0.5 Hz for noncontact images and at 1 Hz for contact images, using constant force in all scans.

In this instrument, samples are attached to a piezoelectric mount and rastered in a rocking motion beneath the scanning tip. Height variations of the sample are detected via laser reflection off the back of the gold-coated cantilever onto a position-sensitive photodiode detector. In contact mode, the repulsive interactions between tip and sample are detected by deflection of the cantilever as the tip traverses the sample. A feedback loop from the detector to the piezo mount adjusts the sample height to maintain a constant cantilever deflection (constant tip force) during the scan. In the "noncontact" mode, the attractive van der Waals interactions between tip and surface are sampled by a highly sensitive modulation technique (Martin et al., 1987; Wiegräbe et al., 1991; Hartmann, 1992). First, a natural resonance frequency of the cantilever is determined at a distance far from the sample surface. The cantilever is then vibrated at this resonance frequency at a fixed amplitude. As the tip approaches the sample, the small force gradients of the surface field shift the resonance frequency of the cantilever. This effect is detected as a change in vibration amplitude at the calibrated frequency. By driving the feedback system to maintain a constant resonance amplitude, the cantilever resonates ~50 Å above the sample surface. This detection technique exerts orders of magnitude less force on the sample than the standard contact mode.

Tips made of silicon and silicon nitride (Park Scientific Instruments, Sunnyvale, CA) were used to image the arrays. The UltraLever and MicroLever have curvature radii of roughly 100 Å and 400 Å, respectively. Tips were discarded when it was determined that they adhered to the surface at the lowest force setting, presumably from protein adsorbed to the tip. Pure silicon tips (UltraLevers) adhered to the surface after only a few scan lines, and were therefore used only in noncontact applications. Contact forces were minimized during scanning by reducing the tip force until contact with the surface was lost. The force was then raised incrementally until stable images were obtained.

To ensure a quantitative analysis of surface topography, the piezo stage was calibrated for vertical accuracy twice within the scanning period using a 600 Å height standard (correct within 10% of our observed sample height). A lateral calibration was performed using a 9.9-μm and a 1-μm standard grid.

Data analysis

Images were deconvolved from raw data to correct for scan distortions (see below) and the effect of tip resolution. For the larger scans, the rock of the

piezo tube added a considerable curvature to the image profile. Scan areas of 100 × 100 μm were fit to a third order polynomial to remove the baseline curvature. Scans smaller than 10 × 10 μm were fit to a first and zero order polynomial to remove tilt and tracking errors. The data presented here are the product of third (if necessary), first, and zero order deconvolutions. These manipulations affect the absolute image height but not the relative feature heights within the image.

Line analysis was performed on all images to quantitate the surface topography. This method is preferable to region analysis, as the "baseline" between scan lines can vary by as much as 10 Å. (This tracking problem is a limitation of the scanning technique over large areas, which is not eliminated by the zero order deconvolution.) Therefore, measurements were taken along the scanning axis to ensure a self-consistent baseline. For the higher resolution scans, values for surface roughness (standard deviation in height) were comparable using line and region analysis. To be consistent, all values of the mean height and standard deviation are reported from the line analysis.

To extract the contribution of the tip profile from the observed feature width, a final deconvolution was performed on the data from the high-resolution protein image. An estimate of the diameter of individual streptavidin molecules was obtained using a deconvolution method that assumes tangential contact between a spherical surface feature and a paraboloid tip (Thundat et al., 1992).

RESULTS

The AFM image in Fig. 2 presents a noncontact scan of an 8 × 8 μm checkerboard-patterned streptavidin array, taken with a 100 Å profile tip at 470 Å lateral pixel resolution. The specificity of streptavidin binding to the 8 μm biotin array is detected with striking clarity. The highly uniform lawn of protein terminates at the edge of biotin derivatization, with

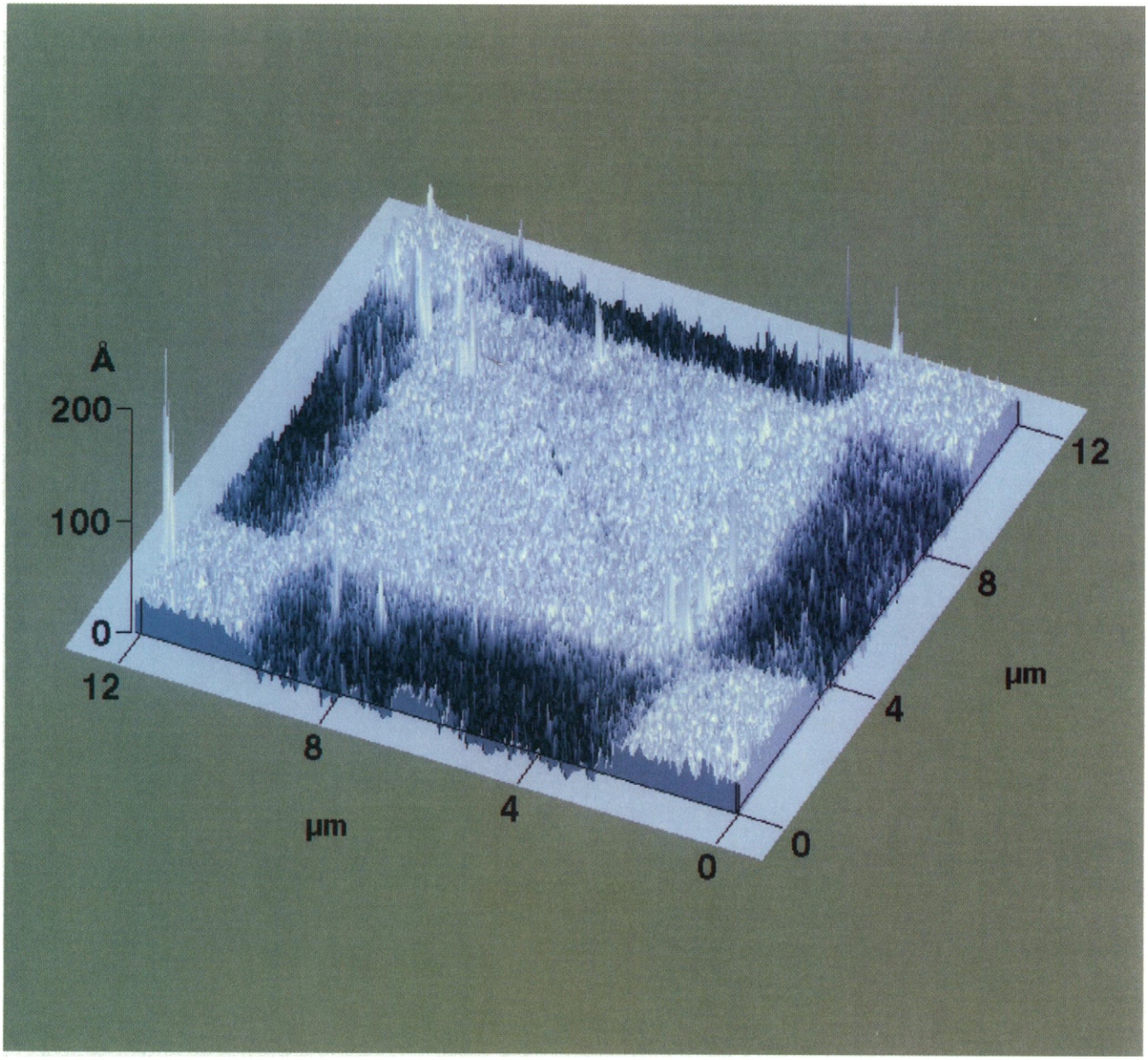

FIGURE 2 Noncontact scan of an 8-μm streptavidin array, taken at 470 Å pixel resolution. The lighter hue corresponds to taller features (protein). Streptavidin binds with high specificity to the biotin regions, with a height of ~35 Å over the underivatized regions. The large spikes seen in this image are indicative of poor tracking response of the feedback loop.

little or no protein detected in the non-derivatized regions. The surface roughness of the array measures 5.3 Å in the areas devoid of protein; the corresponding roughness within the protein elements is 2.7 Å. The protein rises 35 ± 6 Å relative to the underivatized regions. Furthermore, substructure is observed within the protein regions.

A higher resolution scan of one element of the array is shown in Fig. 3 with pixels at 40 Å lateral resolution. The image shows the transition from a derivatized to an underi vatized region of the array. This ~350 nm transition region is defined by the density gradient of streptavidin at the edge of the biotinylated array. A dense, granular topography is evident within the interior of the protein region, which resolves to isolated globular features at the extreme edge of the array. These individual features typically have a 35–45 Å height with a diameter of roughly 250 Å. At the higher resolution, the surface roughness within the protein lawn is 4 Å, with 6 Å deviation in the underivatized regions.

The image in Fig. 4 was obtained by placing the AFM tip in the center of the 8 × 8 μm streptavidin region. The topography was imaged at 15 Å lateral resolution. The lawn of protein is resolved as a close packing of globular features, with an average peak-to-peak spacing of 300 Å. The surface is not uniformly smooth; the protein molecules appear to form an uneven layer with a regional surface roughness of ±5Å. The bright feature appearing in the lower left corner

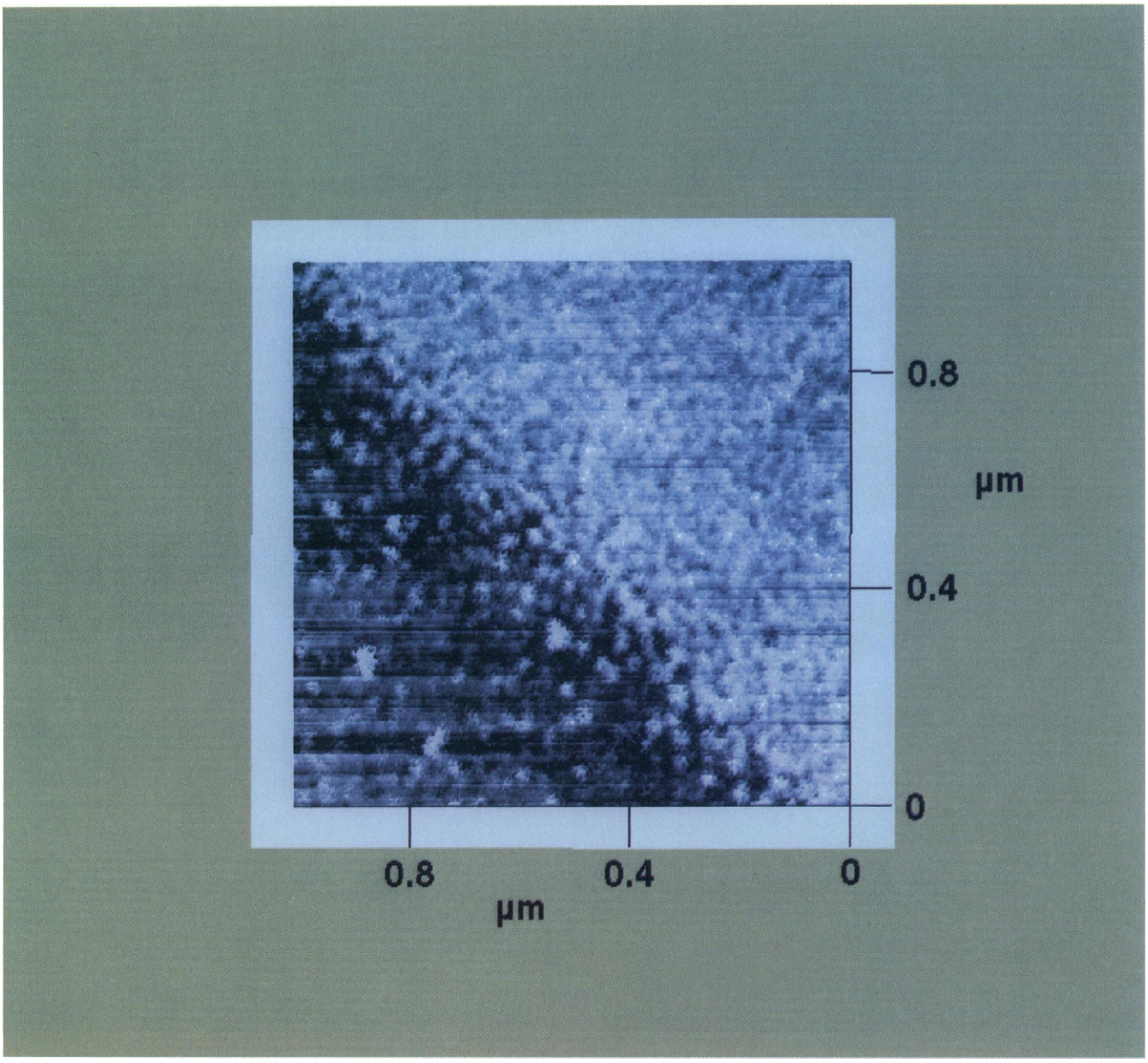

FIGURE 3 Noncontact scan of the edge of the streptavidin-biotin array, taken at 40 Å pixel resolution. Isolated globular features seen at low density are 35–45 Å high with a diameter of roughly 250 Å.

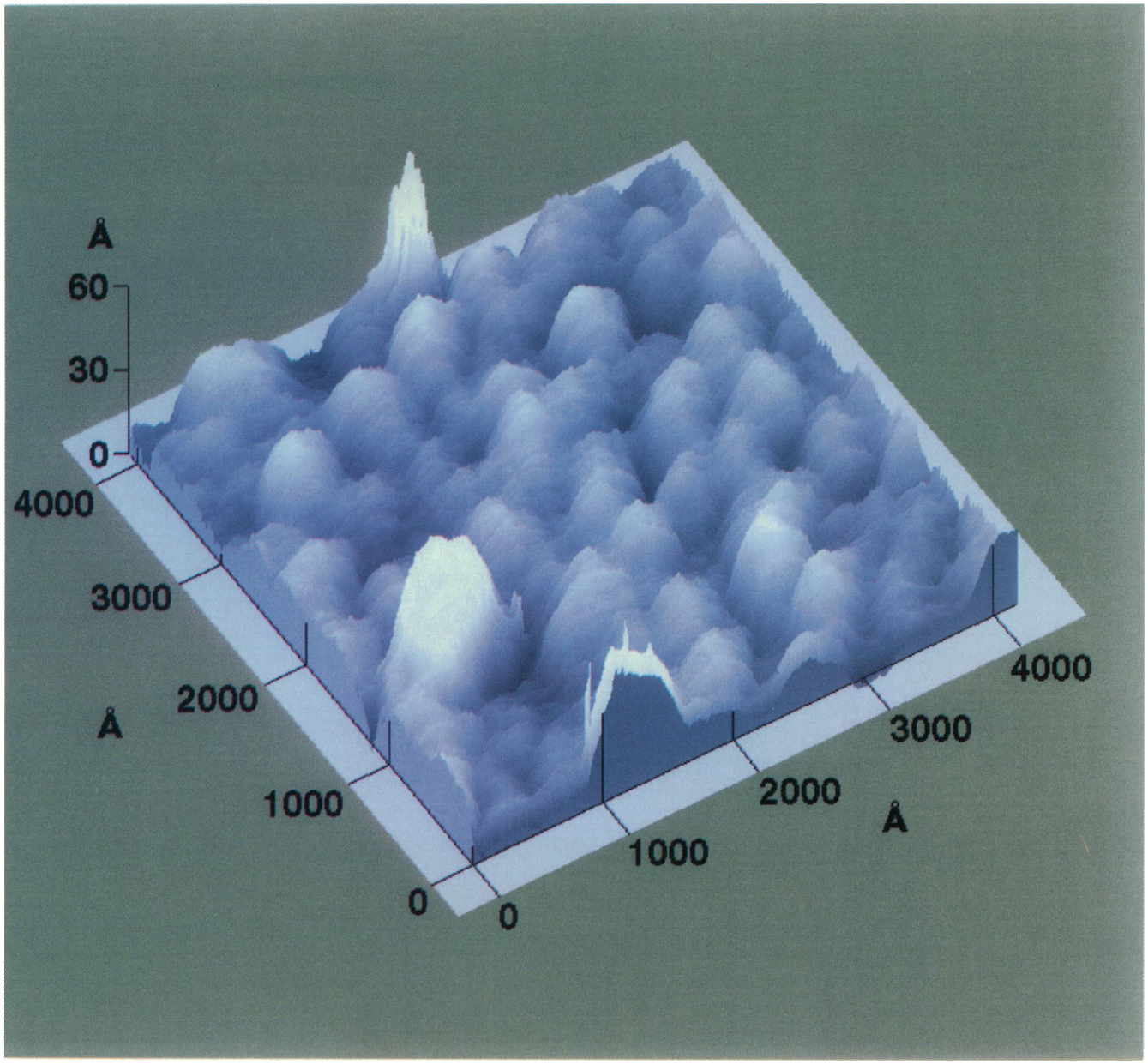

FIGURE 4 Noncontact scan centered within the streptavidin region of Fig. 3, at 17 Å pixel resolution. The protein surface is composed of globular features spaced ~300 Å apart. The bright feature in the lower left corner is probably protein nonspecifically bound to the array.

of the image rises 35 Å above the average height of the surface, and is likely to be streptavidin nonspecifically bound to the protein array. Images taken in this region were reproducible with multiple scans, indicating that the surface was stable and not disrupted by the AFM probe.

The contact scanning tip can be used to modify specific regions of the protein array by using forces strong enough to etch the protein from the substrate. Previous results have demonstrated removal of protein nonspecifically bound to mica (Lee et al., 1994). Fig. 5 presents the tip-directed etching of streptavidin from the covalently bound biotin ligand. In this experiment, a 10 μm clearing was produced in the protein surface by repeated scans at the highest possible force, using a 400 Å aspect ratio tip. After several high-force scans, the encompassing area was scanned at a decreased force to reveal the 10 μm clearing at the edge of the 100 $\times$ 100 μm protein element. Presumably, the dislodged protein was adsorbed to the scanning tip, as no buildup of protein appears on either side of the clearing. The lower left half of the clearing falls on an underivatized element of the array, which is indistinguishable from the underivatized, protein-free areas adjacent to the clearing. However, the upper corner of the cleared region retains an 8 Å height difference over the underivatized area. This height difference may reflect the underlying covalently bound biotin, undisturbed by the scanning tip. The surface roughness of the PEG linker and biotin-capped species is 5.3 Å and 5.2 Å, respec-

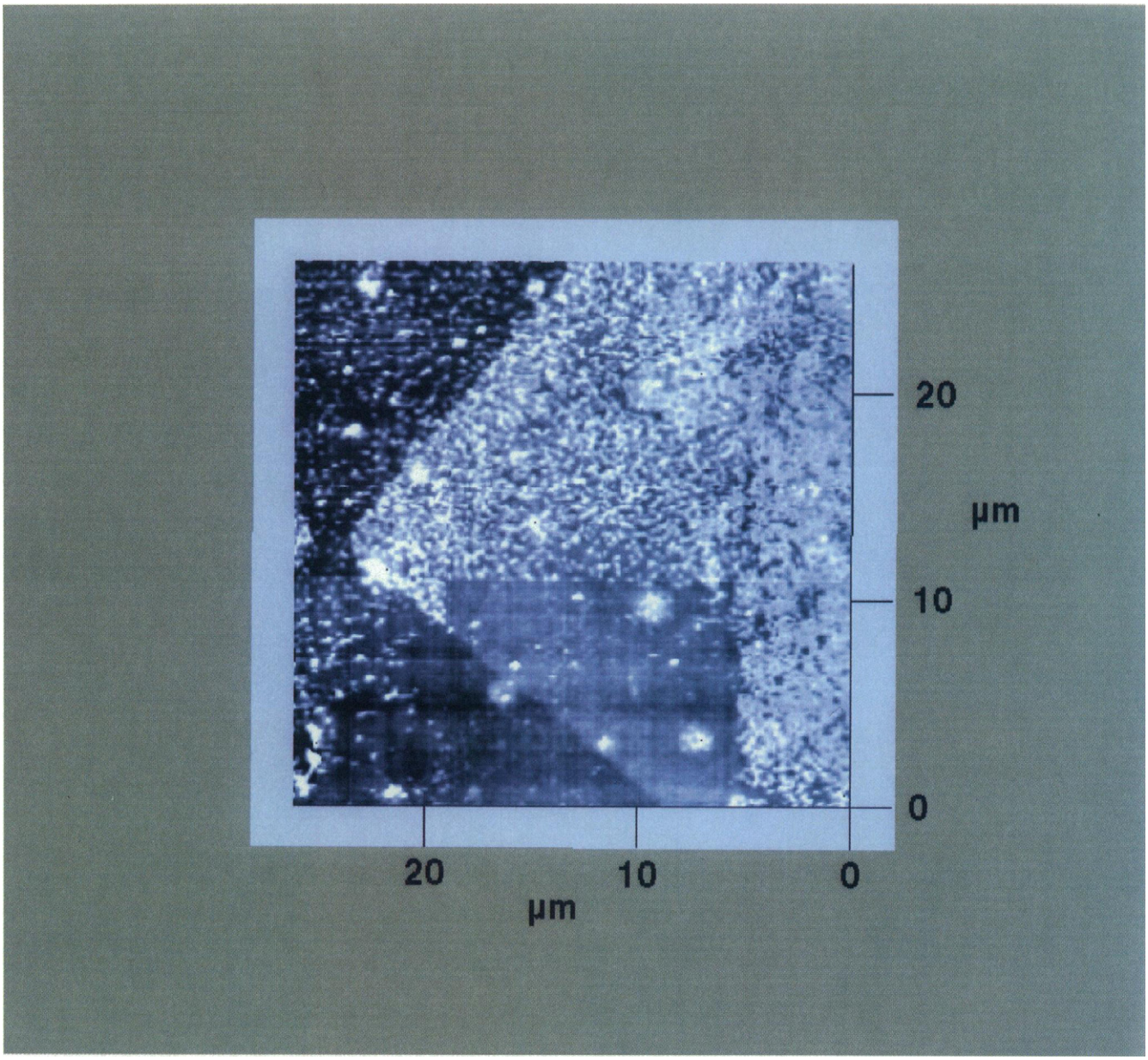

FIGURE 5 AFM tip-directed etching of the streptavidin array. A 10 μm × 10 μm clearing was produced by repeated contact scans at the highest tip force. The encompassing area was then scanned at low force, revealing the 10 μm × 10 μm clearing at the edge of a protein element. The upper right half of the clearing retains an 8 Å height over the underivatized region, probably because of the underlying biotin derivatization.

tively, indicating equivalent topographies within the resolution of these experiments.

DISCUSSION

We have demonstrated that AFM can be used to detect the binding of a receptor to a two-dimensional ligand array. The AFM images reveal streptavidin bound with high specificity to the biotinylated regions of the substrate, with little nonspecific binding in the underivatized areas. The streptavidin regions have a dense, granular topography at low resolution. At higher resolution, the structure is resolved as a dense lawn of globular features with a height of 40 ± 4 Å over the underivatized baseline.

This observed height is close to the 50 Å value predicted by the crystal structure of streptavidin (Hendrickson et al., 1989) and other data from immobilized streptavidin experiments (Darst et al., 1991; Vaknin et al., 1991; Schmidt et al., 1992; Leckband et al., 1994). Since the biotin ligand is encased within the binding pocket of streptavidin (Hendrickson et al., 1989), it is reasonable to assume that this height reflects the dimensions of the protein, which strongly suggests that a monolayer of streptavidin is bound to the ligand array. The height difference between the observed and predicted value may be due to compression of the sample by the AFM tip, as observed in similar experiments using biotinylated lipid bilayers (Weisenhorn et al., 1992). However since little or no distortion is expected with the piconewton forces

applied in the noncontact scanning mode, the difference in height is more likely due to protein dehydration during sample preparation.

At higher resolution, isolated globular features are resolved at the edge of the streptavidin array. We speculate that these features are single molecules of streptavidin, ~40 Å high with a 250 Å diameter. As discussed above, this height argues strongly against aggregation in the vertical dimension. However, the width of these features greatly exceeds the 55 × 45 Å lateral dimensions determined from the x-ray and electron diffraction images of streptavidin (Hendrickson et al., 1989; Darst et al., 1991). Lateral aggregation of the protein could account for the observed width; however, in this case one would expect a range of molecular aggregates within the 100 Å resolution of the tip (i.e., features of 250, 200, 150, and 100 Å width). Since there is no clear evidence of features smaller than 250 Å in these images, we suggest instead that the image is the convolution of a single streptavidin molecule and the 100 Å tip. It has been shown that the AFM tip can significantly broaden the image of features smaller than the tip profile (Thundat et al., 1992), and that a reasonable estimate of the true width can be obtained by deconvolving the tip profile from the image width. For a tip aspect ratio of 100 Å, we obtain a diameter of roughly 60 Å for the isolated features. This number compares favorably to the ~50 Å lateral dimensions of the crystal structure of streptavidin.

The density of the immobilized protein can be determined from the peak-to-peak measurements of the features in Fig. 4. For the measured 300 Å spacing, the density of streptavidin is roughly 10^3 molecules/μm^2. This number is 10-fold less than the density expected for close packing of streptavidin, or from the expected density of biotin sites (both ~10^4 molecules/μm^2). This may result from incomplete coupling of the linker and/or biotin moieties; however, these data were consistent for different synthesis protocols (as mentioned earlier, surfaces were derivatized using 50 mM and 100 mM linker solutions. Alternatively, the irregular ligand topography may render sites inaccessible for protein binding. In each image, the surface roughness of the protein is less than that of the underlying substrate. Because the streptavidin structure is larger than biotin, the protein may sample only the extended species of the ligand. This effect would reduce the expected density of protein bound to the array. At any rate, the observed density of streptavidin is probably not sufficient to allow two-dimensional crystallization as has been observed in lipid monolayer systems (Darst et al., 1991).

The AFM scans reflect the resolution of the photolithographic process used to create the arrays. The 350 nm density gradient observed at the edge of each derivatization element is most likely due to the diffraction of light at the edge of the mask during photolysis. In the diffraction zone, the less intense light produces a lower density of activated sites for ligand attachment. The 350-nm zone suggests that, under these photolysis conditions, elements should have at least 1 μm separation for adequate resolution from the baseline substrate. Somewhat higher photolithographic resolution might be achieved using noncontact lithographic techniques or by using laser photolysis; however, it is clear that the resolving power of the AFM far exceeds the limits of conventional lithography. More advanced near-field techniques may be investigated to drive the resolution of derivatization. For example, a modified probe such as the near-field scanning optical microscope has been used for photobleaching at molecular resolution (Ambrose et al., 1994) and may prove applicable for molecular photolithography.

The ability of the atomic force probe to directly interact with surface molecules suggests applications in quantitative surface analysis. For example, the tip can be derivatized with a ligand (or receptor) and then applied to its surface-immobilized complement to probe energies of affinity and adhesion (Nakagawa et al., 1993; Florin et al., 1994; Lee et al., 1994). The force required for mechanical dissociation of the complementary pair should reflect to the free energy or enthalpy of a single molecular interaction. These measurements may provide an insightful comparison to the bulk thermodynamic energies sampled by conventional solution experiments.

CONCLUSION

We have demonstrated a powerful combination of techniques to fabricate and detect biological arrays. Photolithography was used to direct the synthesis of a matrix of biological ligands, which serves as a well-defined substrate to immobilize biological macromolecules such as proteins. AFM was then used to detect affinity-bound protein. In addition, we have shown that the protein array can serve as a template for selective etching using the AFM tip, which may be used to selectively engrave a sub-lattice within the deposited array. Furthermore, it may be possible to extend this capacity to include tip-directed chemistry by physically removing protecting groups, inducing chemical catalysis, or by delivering reactants to precise locations on the array. The ability to microfabricate biological elements, in combination with new applications of AFM, shows potential as a unique medium for the study of biomolecular interactions.

We wish to thank James Winkler for his expertise in high resolution lithography, and Dr. Xiaohua Huang for his assistance in fabricating the biotin arrays.

REFERENCES

Ambrose, W. P., P. M. Goodwin, J. C. Martin, and R. A. Keller. 1994. Single molecule detection and photochemistry on a surface using near-field optical excitation. *Phys. Rev. Lett.* 72:160–163.

Atkinson, T., and M. Smith. 1984. Solid phase synthesis of oligodexoyribonucleotides by the phosphite-triester method. *In* Oligonucleotide Synthesis: A Practical Approach. M. J. Gait, editor. IRL Press, Oxford, England. 35–81.

Binnig, G., C. F. Quate, and C. Gerber. 1986. Atomic force microscope. *Phys. Rev. Lett.* 56:930–933.

Blackford, B. L., M. H. Jericho, and P. J. Mulhern. 1991. A review of scanning tunneling microscope and atomic force microscope imaging of large biological structures: problems and prospects. *Scanning Microsc.* 5:907–918.

Darst, S. A., M. Ahlers, P. H. Meller, E. W. Kubalek, R. Blankenburg, H. O. Ribi, H. Ringsdorf, and R. D. Kornberg. 1991. Two dimensional crystals of streptavidin on biotinylated lipid layers and their interactions with biotinylated macromolecules. *Biophys. J.* 59:387–396.

Drake, B., C. B. Prater, A. L. Weisenhorn, S. A. C. Gould, T. R. Albrecht, C. F. Quate, D. S. Cannell, H. G. Hansma, and P. K. Hansma. 1989. Imaging crystals, polymers and processes in water with the atomic force microscope. *Science (Washington DC).* 243:1586–1588.

Florin, E.-L., V. T. Moy, and H. E. Gaub. 1994. Adhesion forces between individual ligand-receptor pairs. *Science (Washington DC).* 264:415–417.

Fodor, S. P. A., J. L. Read, M. C. Pirrung, L. Stryer, A. Tsai Lu, and D. Solas. 1991. Light-directed, spatially addressable parallel chemical synthesis. *Science (Washington DC).* 260:1649–1652.

Hansma, P. K., V. B. Elings, O. Marti, and C. E. Bracker. 1988. Scanning tunneling microscopy and atomic force microscopy: application to biology and technology. *Science (Washington DC).* 242:209–216.

Hartmann, U. 1992. Intermolecular and surface forces in noncontact scanning force microscopy. *Ultramicroscopy.* 42–44:59–65.

Hendrickson, W. A., A. Pähler, J. L. Smith, Y. Satow, E. A. Merritt, and R. P. Phizackerley. 1989. Crystal structure of core streptavidin determined from multiwavelength anomalous diffraction of synchrotron radiation. *Proc. Natl. Acad. Sci. USA.* 86:2190–2194.

Ill, C. R., V. M. Keivens, J. E. Hale, K. K. Nakamura, R. A. Jue, S. Cheng, E. D. Melcher, B. Drake, and M. C. Smith. 1993. A COOH-terminal peptide confers regiospecific orientation and facilitates atomic force microscopy of an IgG_1. *Biophys. J.* 64:919–924.

Karrasch, S., M. Dolder, F. Schabert, J. Ramsden, and A. Engel. 1993. Covalent binding of biological samples to solid supports for scanning probe microscopy in buffer solution. *Biophys. J.* 65:2437–2446.

Keller, D., and C. Bustamante. 1993. Attaching molecules to surfaces for scanning probe microscopy. *Biophys. J.* 64:896–897.

Leckband, D. E., F.-J. Schmitt, J. N. Israelachvili, and W. Knoll. 1994. Direct force measurements of specific and nonspecific protein interactions. *Biochemistry.* 33:4611–4624.

Lee, G. U., D. A. Kidwell, and R. J. Colton. 1994. Sensing discrete streptavidin-biotin interactions with atomic force microscopy. *Langmuir.* 10:354–357.

Lin, J. N., B. Drake, A. S. Lea, P. K. Hansma, and J. D. Andrade. 1990. Direct observation of immunoglobulin adsorption dynamics using the atomic force microscope. *Langmuir.* 6:509–511.

Martin, Y., C. C. Williams, and H. K. Wickramasinghe. 1987. Atomic force microscope-force mapping and profiling on a sub 100-Å scale. *J. Appl. Physiol.* 61:4723–4729.

Nakagawa, T., K. Ogawa, T. Kurumizawa, and S. Ozaki. 1993. Discriminating molecular length of chemically adsorbed molecules using an atomic force microscope having a tip covered with sensor molecules (an atomic force microscope having chemical sensing function). *Jpn. J. Appl. Physiol.* 32:L294–296.

Pease, A. C., D. Solas, E. J. Sullivan, M. T. Cronin, C. P. Holmes, and S. P. A. Fodor. 1994. Light-generated oligonucleotide arrays for rapid DNA sequence analysis. *Proc. Natl. Acad. Sci. USA.* 91:5022–5026.

Radmacher, M., R. W. Tillmann, M. Fritz and H. E. Gaub. 1992. From molecules to cells: imaging soft samples with the atomic force microscope. *Science (Washington DC).* 257:1900–1905.

Schmidt, A., J. Spinke, T. Bayerl, E. Sackmann, and W. Knoll. 1992. Streptavidin binding to biotinylated lipid layers on solid supports. *Biophys. J.* 63:1185–1192.

Shaiu, W.-L., D. D. Larson, J. Vesenka, and E. Henderson. 1993. Atomic force microscopy of oriented linear DNA molecules labeled with 5 nm gold spheres. *Nucleic Acids Res.* 21:99–103.

Thundat, T., X.-Y Zheng, S. L. Sharp, D. P. Allison, R. J. Warmack, D. C. Joy, and T. L. Ferrell. 1992. Calibration of atomic force microscope tips using biomolecules. *Scanning Microsc.* 6:903–910.

Vaknin, D., J. Als-Nielsen, M. Piepenstock, and M. Lösche. 1991. Recognition processes at a functionalized lipid surface observed with molecular resolution. *Biophys. J.* 60:1545–1552.

Weisenhorn, A. L., B. Drake, C. B. Prater, S. A. C. Gould, P. K. Hansma, F. Ohnesorge, M. Egger, S.-P. Heyn, and H. E. Gaub. 1990. Immobilized proteins in buffer imaged at molecular resolution by atomic force microscopy. *Biophys. J.* 58:1251–1258.

Weisenhorn, A. L., P. K. Hansma, T. R. Albrecht, and C. F. Quate. 1989. Forces in atomic force microscopy in air and water. *Appl. Phys. Lett.* 54:2651–2653.

Weisenhorn, A. L., F.-J. Schmitt, W. Knoll, and P. K. Hansma. 1992. Streptavidin binding observed with an atomic force microscope. *Ultramicroscopy.* 42–44:1125–1132.

Wiegräbe, W., M. Nonnenmacher, R. Guckenberger, and O. Wolter. 1991. Atomic force microscopy of a hydrated bacterial surface protein. *J. Microsc. (Oxf.)* 163:79–84.

Zenhausern, F., M. Adrian, B. ten Heggeler-Bordier, F. Ardizzoni, and P. Descouts. 1993. Enhanced imaging of biomolecules with electron beam deposited tips for scanning force microscopy. *J. Appl. Physiol.* 73:7232–7237.